

Activation cross-sections of longer lived products of deuteron induced nuclear reactions on ytterbium up to 40 MeV

F. Tárkányi^a, F. Ditrói^{a,*}, S. Takács^a, A. Hermanne^b, H. Yamazaki^c, M. Baba^c, A. Mohammadi^c, A.V. Ignatyuk^d

^a Institute for Nuclear Research of the Hungarian Academy of Sciences (ATOMKI), Debrecen, Hungary

^b Cyclotron Laboratory, Vrije Universiteit Brussel (VUB), Brussels, Belgium

^c Cyclotron Radioisotope Center (CYRIC), Tohoku University, Sendai, Japan

^d Institute of Physics and Power Engineering (IPPE), Obninsk, Russia

ARTICLE INFO

Article history:

Received 21 February 2013

Available online 13 April 2013

Keywords:

^{nat}Yb target

Deuteron induced reactions

^{177,173,172mg,171mg,170,169}Lu

^{175,169}Yb

^{173,172,168,167,165}Tm activation products

Cross-section

Integral yields

Theoretical calculations

ABSTRACT

In the frame of a systematic study of the activation cross-sections of the deuteron induced nuclear reactions, excitation functions of the ^{nat}Yb(*d*,xn)^{177,173,172mg,171mg,170,169}Lu, ^{nat}Yb(*d*,x)^{175,169}Yb and ^{nat}Yb(*d*,x)^{173,172,168,167,165}Tm reactions are studied up to 40 MeV, a few of them for the first time. Cross-sections were measured with the activation method using a stacked foil irradiation technique and high resolution γ -ray spectrometry. The experimental data are analyzed and compared to the results of the theoretical model codes ALICE-IPPE, EMPIRE-II and TALYS. From the measured cross-section data integral production yields were calculated. Applications of the new cross-sections are discussed.

© 2013 Elsevier B.V. All rights reserved.

1. Introduction

Activation cross-sections data of deuteron induced nuclear reactions are important both for application in several fields and for benchmarking description of reactions with different model codes. In connection with several projects it was recognized that a high priority needs to be given to establish a reliable database for deuteron activation data. Literature search shows that the status of the available cross-section data for deuteron induced reactions (especially above 15–20 MeV) is very poor. No systematical study has been done earlier and the cross-section data (except a few well measured monitor and medically important reactions) show large discrepancies.

To meet the requirement of improving the reliability of available data, we started to establish an experimental activation database some years ago, by performing new experiments and a systematical survey of published deuteron induced activation cross-sections up to 50 MeV. The targets were irradiated with external beams of the Debrecen, Brussels, Louvain-la-Neuve, and Sendai cyclotrons. The mostly new, measured excitation functions

are compared with the results of different nuclear reaction model codes.

As a continuation of our investigation of deuteron induced activation cross-sections on rare earth targets we performed an irradiation of Yb targets with a 40 MeV incident deuteron beam at the Sendai cyclotron. Due to the experimental circumstances (rather long cooling times before start of activity measurement) this experiment results in excitation functions for longer lived Yb, Lu and Tm radionuclides. We have already earlier experimentally studied most of these activation products in proton and alpha-particle induced nuclear reactions on ytterbium [1–3].

2. Earlier investigations

Only a few earlier experimental works have been found dealing with deuteron induced activation products on Yb, mostly at lower energies.

- Nichols et al. investigated the excitation functions of Yb(*d*,xn)¹⁷¹Lu,¹⁷²Lu,¹⁷³Lu between 13.4 and 29.0 MeV [4].
- Hermanne et al., investigated the cross-sections for deuteron-induced reactions on Yb and measured cross-sections between 3 and 20 MeV for Yb(*d*,xn)¹⁷⁰Lu/¹⁷¹Lu/¹⁷²Lu/¹⁷³Lu/¹⁷⁴Lu/¹⁷⁷Lu, and Yb(*d*,xnp)¹⁶⁹Yb/¹⁷⁵Yb [5].

* Corresponding author.

E-mail address: ditroi@atomki.hu (F. Ditrói).

- Manenti et al. measured the activation cross-sections of $\text{Yb}(d,xn)^{169}\text{Lu}/^{170}\text{Lu}/^{171}\text{Lu}/^{172}\text{Lu}/^{173}\text{Lu}/^{174}\text{Lu}/^{176}\text{Lu}/^{177}\text{Lu}$, $\text{Yb}(d,xnp)^{169}\text{Yb}/^{175}\text{Yb}/^{177}\text{Yb}$ reactions up to 18.18 MeV [6].
- Dmitriev et al., in the frame of a systematic study: “Yields of Radioactive Nuclides Formed by Bombardment of a Thick Target with 22-MeV Deuterons” measured the thick target yields on Yb for production of $^{173,174}\text{Lu}$ [7].

Considering the theoretical results on production cross-sections for deuteron induced reactions on different target material we have found also only few works:

- Results calculated by the ALICE-IPPE code [8] can be found in [5].
- The most recent results of systematic calculations made by the TALYS code [9] can be found in the TENDL 2012 on line library [10].
- Comparison of evaluated and experimental data from ENDF/B-VII.1, TENDL-2011 and EXFOR can be found in the JANIS Book of deuteron-induced cross-sections prepared by Soppera et al [11].

3. Experimental

Elemental cross-sections on ^{nat}Yb targets were measured using the activation method and the standard stacked foil irradiation technique combined with high-resolution γ -ray spectrometry. The irradiation, the activity measurement and the data evaluation were similar as described in more detail in our recent works [12].

The excitation functions were measured up to 40 MeV by bombarding ^{nat}Yb targets with low intensity deuteron beams at the AVF-930 cyclotron of the Tohoku University (Sendai). Reactions induced on Al foils present in the stack were used to monitor the parameters of the bombarding deuteron beams.

The ytterbium (thickness 23 μm) and aluminum foils (thickness 100 μm) were of high purity (>99.5%) and purchased from Goodfellow (UK).

The irradiated stack had a complex structure, consisting of a nine times repeated sequence of Rh(12.3 μm), Ho(25 μm), Au(10.7 μm), Yb(23 μm), MoRe alloy(50 μm), CuMnNi alloy(25 μm) foils and the Al(100 μm) foils serving as monitor.

In principle (n,γ) and $(n,2n)$ reactions induced by secondary neutrons can also contribute to the production of the isotopes of Yb. We have checked the possible effect of neutron induced reactions by inserting additional target foils at the end of the stack holder, where complete stopping of the deuterons is expected. In the used irradiation setup the effect of neutrons was found to be negligibly small.

The results for the Mn, Rh, Au and MoRe targets were already published [12–15] and for Ho and Ni target material will be discussed in separate reports.

The irradiation of the targets was performed in He-gas atmosphere in a water cooled target holder. For determination of the beam intensity and energy, the complete excitation functions of the $^{27}\text{Al}(d,x)^{22,24}\text{Na}$ monitor reactions were measured, simultaneously with the excitation functions of reactions induced on Yb targets (see Fig. 1). The target stack was irradiated with a collimated deuteron beam of 40 MeV incident energy, for 30 min at about 24 nA.

The radioactivity of each sample and monitor foil was assessed nondestructively by HPGe γ -spectrometry in two series of measurements. The first counting series was started about 20 h after the end of the bombardment (EOB) (each foil was measured for 10 min), the second series started about 20 days after EOB (each foil was measured for 5–8 h). The large number of irradiated foils and the high induced activity prevented the optimization of the spectrum measurements of the samples. The information on activity of short-lived radionuclides was lost due to initial one day waiting time after EOB. Due to the large number of foils and the limited number of detectors (2), the measuring time of the first assessment was restricted to 10 min. An additional inconvenience of these circumstances is that detection of the weak γ -lines of medium half-life radioisotopes was also impossible.

The decay data were taken from NUDAT 2.6 [16], the standard cross-section data of the used monitor reactions $^{nat}\text{Al}(p,x)^{22,24}\text{Na}$ from IAEA recommended database [17]. For the reaction Q -values we used the NNDC Q -value calculator [18]. The energy degradation along the stack was determined via calculation [19] and corrected on the basis of the simultaneously measured monitor reactions by the method described in [20]. The excitation functions were hence

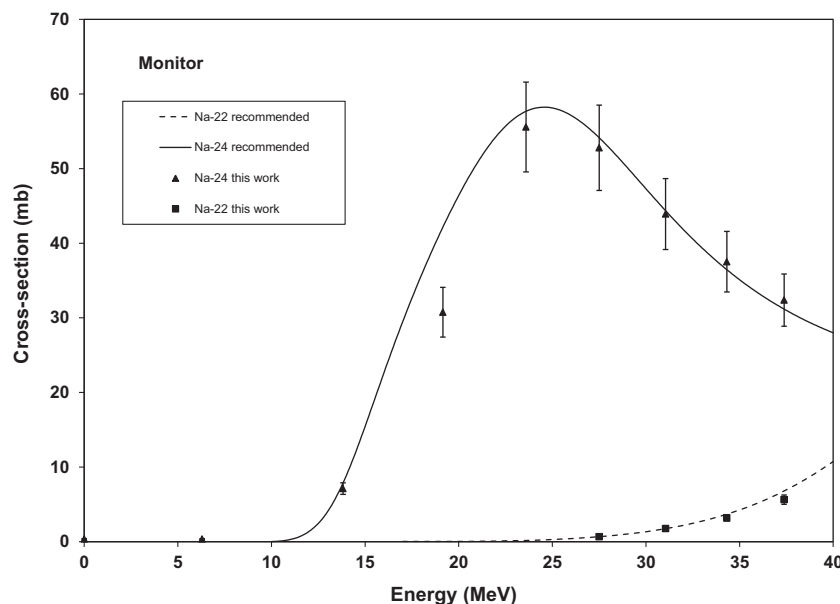


Fig. 1. Application of monitoring using the $^{27}\text{Al}(d,x)^{22,24}\text{Na}$ reaction.

Table 1
Decay characteristic of the investigated reaction products.

| Nuclide | Half-life | E_{γ} (keV) | I_{γ} (%) | Contributing reaction | Q-value (keV) |
|--------------------|-----------|--------------------|------------------|---------------------------|---------------|
| ^{177g}Lu | 6.647 d | 112.9498 | 6.17 | $^{176}\text{Yb}(d,n)$ | 3959.3 |
| | | 208.3662 | 10.36 | ^{177}Yb decay | |
| ^{173}Lu | 1.37 y | 78.63 | 11.9 | $^{172}\text{Yb}(d,n)$ | 2689.9 |
| | | 100.724 | 5.24 | $^{173}\text{Yb}(d,2n)$ | –3677.41 |
| | | 272.105 | 21.2 | $^{174}\text{Yb}(d,3n)$ | –11142.05 |
| | | | | $^{176}\text{Yb}(d,5n)$ | –23829.22 |
| ^{172g}Lu | 6.70 d | 78.7426 | 10.6 | $^{171}\text{Yb}(d,n)$ | 2493.6 |
| | | 181.525 | 20.6 | $^{172}\text{Yb}(d,2n)$ | –5525.86 |
| | | 810.064 | 16.6 | $^{173}\text{Yb}(d,3n)$ | –11893.17 |
| | | 900.724 | 29.8 | $^{174}\text{Yb}(d,4n)$ | –19357.81 |
| | | 912.079 | 15.3 | $^{176}\text{Yb}(d,6n)$ | –32044.98 |
| | | 1093.63 | 63 | | |
| ^{171g}Lu | 8.24 d | 667.422 | 11.1 | $^{170}\text{Yb}(d,n)$ | 2128.98 |
| | | 739.793 | 47.9 | $^{171}\text{Yb}(d,2n)$ | –4485.5 |
| | | 780.711 | 4.37 | $^{172}\text{Yb}(d,3n)$ | –12504.96 |
| | | 839.961 | 3.05 | $^{173}\text{Yb}(d,4n)$ | –18872.29 |
| | | | | $^{174}\text{Yb}(d,5n)$ | –26336.93 |
| | | | | $^{176}\text{Yb}(d,7n)$ | –39024.1 |
| ^{170}Lu | 2.012 d | 84.262 | 8.7 | $^{170}\text{Yb}(d,2n)$ | –6465.7 |
| | | 193.13 | 2.07 | $^{171}\text{Yb}(d,3n)$ | –13080.2 |
| | | 572.20 | 1.25 | $^{172}\text{Yb}(d,4n)$ | –21099.6 |
| | | 985.10 | 5.4 | $^{173}\text{Yb}(d,5n)$ | –27466.9 |
| | | 1054.28 | 4.60 | $^{174}\text{Yb}(d,6n)$ | –34931.6 |
| | | 1138.65 | 3.49 | | |
| | | 1280.25 | 7.9 | | |
| | | 1341.20 | 3.15 | | |
| | | 1364.60 | 4.47 | | |
| ^{169}Lu | 32.018 d | 109.77924 | 17.39 | $^{168}\text{Yb}(d,n)$ | 1567.07 |
| | | 130.52293 | 11.38 | $^{170}\text{Yb}(d,3n)$ | –13769.87 |
| | | 177.21307 | 22.28 | $^{171}\text{Yb}(d,4n)$ | –20384.37 |
| | | 197.95675 | 35.93 | $^{172}\text{Yb}(d,5n)$ | –28403.84 |
| | | | | $^{173}\text{Yb}(d,6n)$ | –34771.16 |
| ^{167}Lu | 51.5 m | 178.87 | 2.5 | $^{168}\text{Yb}(d,3n)$ | –15151.7 |
| | | 213.20 | 3.33 | $^{170}\text{Yb}(d,5n)$ | –30488.7 |
| | | 239.22 | 7.7 | $^{171}\text{Yb}(d,6n)$ | –37103.2 |
| | | 401.17 | 3.17 | $^{172}\text{Yb}(d,7n)$ | –45122.7 |
| | | 1267.26 | 3.87 | | |
| ^{177}Yb | 1.911 h | 150.3 | 20.5 | $^{176}\text{Yb}(d,p)$ | 3341.834 |
| ^{175}Yb | 4.185 d | 113.805 | 3.87 | $^{174}\text{Yb}(d,p)$ | 3597.7842 |
| | | 282.522 | 6.13 | $^{176}\text{Yb}(d,p2n)$ | –9089.38 |
| | | 396.329 | 13.2 | ^{175}Tm decay | |
| ^{169}Yb | 32.018 d | 109.77924 | 0.1739 | $^{168}\text{Yb}(d,p)$ | 4642.414 |
| | | 130.52293 | 0.1138 | $^{170}\text{Yb}(d,p2n)$ | –10694.52 |
| | | 177.21307 | 0.2228 | $^{171}\text{Yb}(d,p3n)$ | –17309.02 |
| | | 197.95675 | 0.3593 | $^{172}\text{Yb}(d,p4n)$ | –25328.49 |
| | | 307.52 | 0.003 | $^{173}\text{Yb}(d,p5n)$ | –31695.81 |
| | | 307.73586 | 0.1005 | $^{174}\text{Yb}(i,p6n)$ | –39160.45 |
| ^{173}Tm | 8.24 h | | | ^{169}Lu decay | |
| | | 398.9 | 87.9 | $^{173}\text{Yb}(d,2p)$ | –2739.62 |
| | | 461.4 | 6.9 | $^{174}\text{Yb}(d,2pn)1$ | –10204.25 |
| ^{168}Tm | 93.1 d | | | $^{176}\text{Yb}(d,2p3n)$ | –22891.43 |
| | | 79.804 | 10.8 | $^{168}\text{Yb}(d,2p)$ | –1699.2 |
| | | 184.295 | 17.9 | $^{170}\text{Yb}(d,2p2n)$ | –17036.15 |
| | | 198.251 | 53.8 | $^{171}\text{Yb}(d,2p3n)$ | –23650.65 |
| | | 447.515 | 23.7 | $^{172}\text{Yb}(d,2p4n)$ | –31670.12 |
| | | 720.392 | 12.0 | $^{173}\text{Yb}(d,2p5n)$ | –38037.44 |
| | | 741.355 | 12.6 | | |
| | | 815.989 | 50.3 | | |
| ^{167}Tm | 9.25 d | 821.162 | 11.8 | | |
| | | 207.801 | 42 | $^{168}\text{Yb}(d,2pn)$ | –8539.87 |
| | | 531.54 | 1.61 | $^{170}\text{Yb}(d,2p3n)$ | –23876.82 |
| | | | | $^{171}\text{Yb}(d,2p4n)$ | –30491.32 |
| | | | | $^{172}\text{Yb}(d,2p5n)$ | –38510.79 |
| | | | | ^{167}Yb decay | |

Table 1 (continued)

| Nuclide | Half-life | E_γ (keV) | I_γ (%) | Contributing reaction | Q-value (keV) |
|-------------------|-----------|------------------|----------------|---------------------------|---------------|
| ^{165}Tm | 30.06 h | 242.917 | 35.5 | $^{168}\text{Yb}(d,2p3n)$ | –24294.89 |
| | | 297.369 | 12.7 | $^{170}\text{Yb}(d,2p5n)$ | –39631.84 |
| | | 460.263 | 4.12 | ^{165}Yb decay | |

Abundance of isotopes in natural Yb (%): ^{168}Yb –0.13, ^{170}Yb –3.05, ^{171}Yb –14.3, ^{172}Yb –21.9, ^{173}Yb –16.12, ^{174}Yb –31.8, ^{176}Yb –12.7.

The Q-values refer to formation of the ground state and are obtained from [18].

When complex particles are emitted instead of individual protons and neutrons the Q-values have to be decreased by the respective binding energies of the compound particles: np–d, +2.2 MeV; 2np–t, +8.48 MeV; n2p– ^3He , +7.72 MeV; 2n2p– α , +28.30 MeV.

determined in an accurate way relative to the simultaneously re-measured monitor reactions.

The decay data and the contributing reactions with their Q-values are presented in Table 1.

The naturally occurring ytterbium is composed of seven stable isotopes, therefore, so called elemental cross-sections were determined except for ^{177}Lu , where only (d,p) and (d,n) reactions on ^{176}Yb can contribute (see Table 1).

The uncertainties on the cross-section values were estimated in the standard way: the independent relative errors of the linearly contributing processes were summed quadratically and the square root of the sum was taken [21]. The uncertainty of the energy of the bombarding beam in the middle of each irradiated foil was estimated combining the uncertainties of the energy degradation depending on the thickness of the target foils in the stack and the energy straggling.

4. Comparison with the results of model codes

The experimental data are compared with the cross-section data reported in the last two TALYS based TENDL 2011 and TENDL 2012 Activation Data Libraries [10] to show the agreement with the experimental data and contribute to the development of the TENDL data library. The cross-sections of the investigated reactions were calculated by us, using the modified pre-compound model codes ALICE-IPPE [8] and EMPIRE-II [22].

In the modified ALICE IPPE-D and EMPIRE-D code versions the direct (d,p) channel is increased strongly, which gives better agreement for the (d,p) channel, but naturally it reflects also in the results for all other reactions [23,24].

5. Results

The measured experimental cross-section data are shown in Figs 2–15 together with the earlier literature results and results of the theoretical calculations. The numerical values are collected in Tables 2 and 3. The following notations were used:

- The “mg” denotes the activation cross-section of the ground state after the “complete” decay of the significantly shorter half-life isomeric state decaying partly or completely to that ground state;
- The “cum” denotes the activation cross-section of the final product after the “complete” decay of the simultaneously produced significantly shorter half-life parent nuclei decaying partly or completely to the investigated final product.

5.1. Cross-sections of lutetium radioisotopes

Except for production of ^{177}Lu only direct (d,xn) reactions contribute to the formation of the measured lutetium radioisotopes.

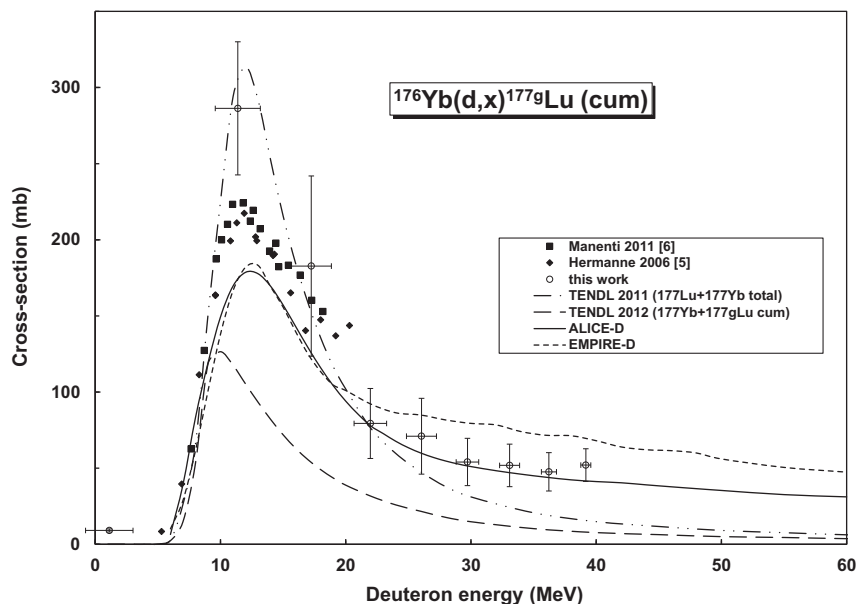


Fig. 2. Excitation function of the $^{176}\text{Yb}((d,x)^{177}\text{Lu})$ process.

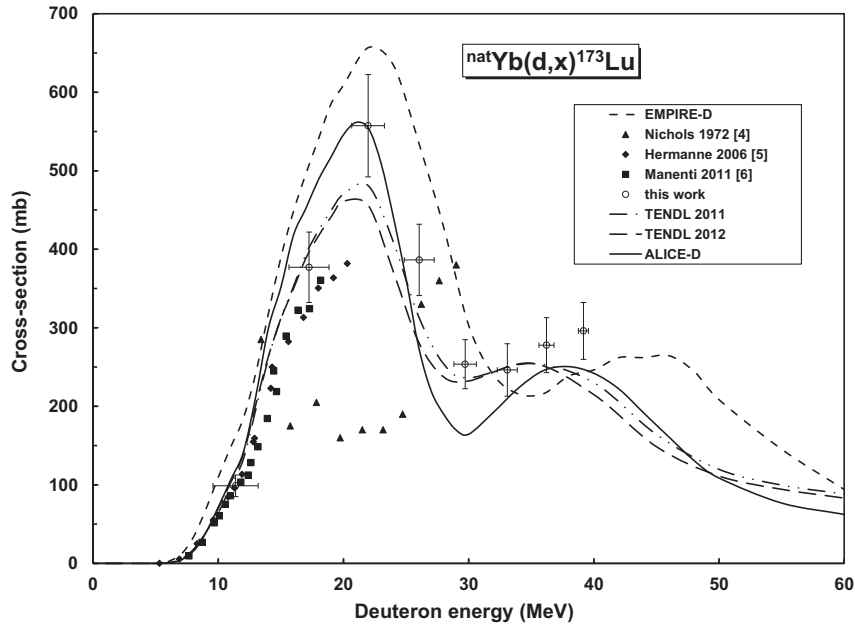


Fig. 3. Excitation function of the $^{nat}\text{Yb}(d,xn)^{173}\text{Lu}$ process.

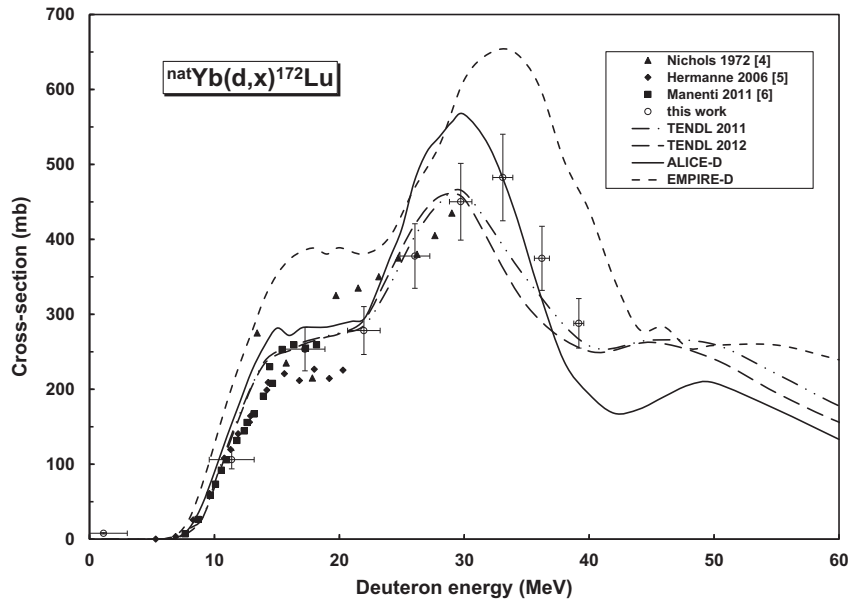


Fig. 4. Excitation function of the $^{nat}\text{Yb}(d,xn)^{172m}\text{Lu}$ process.

5.1.1. $^{176}\text{Yb}(d,xn)^{177}\text{Lu}$

In this study, only the cumulative production of ^{177g}Lu (6.71 d half-life) following total decay of parent ^{177}Yb ($T_{1/2} = 1.9$ h) was assessed. It practically contains no contribution from the internal decay of ^{177m}Lu (160.4 d, IT 21.7%) (long-lived, low formation cross-section).

The medically relevant ^{177g}Lu can be produced in a direct reaction via $^{176}\text{Yb}(d,n)^{177g}\text{Lu}$ or indirectly by decay of parent ^{177}Yb obtained through the $^{176}\text{Yb}(d,p)^{177m+g}\text{Yb}$ route. According to the earlier low-energy measurements [5,6] and to the results of the model calculations, the (d,p) reaction has a significant predominance over the direct (d,n) process. The cross-section data above 20 MeV obtained in this study, have large uncertainties due to the separation process of the 208 keV γ -line of ^{177g}Lu overlapping

with the γ -line at nearly the same energy of ^{167}Tm (with a half-life of 9.25 d, similar to ^{177g}Lu).

Our new data are higher than the literature experimental data in the overlapping energy region (Fig. 2). The TENDL 2011 values present total cross-sections of ^{177}Lu but in the TENDL 2012 already the cumulative cross-section of the ^{177g}Lu can be deduced. Taking into account the small cross-sections of the direct production of the ^{177m}Lu the TENDL 2011 results reproduce well the experimental data, both the shape and the magnitude. In case of the TENDL 2012 the underestimation of the experimental data is significant.

5.1.2. $^{nat}\text{Yb}(d,xn)^{173}\text{Lu}$

The production of ^{173}Lu (1.37 a) arises from reactions on four stable Yb isotopes. The contribution of the $^{172}\text{Yb}(d,n)$ reaction is

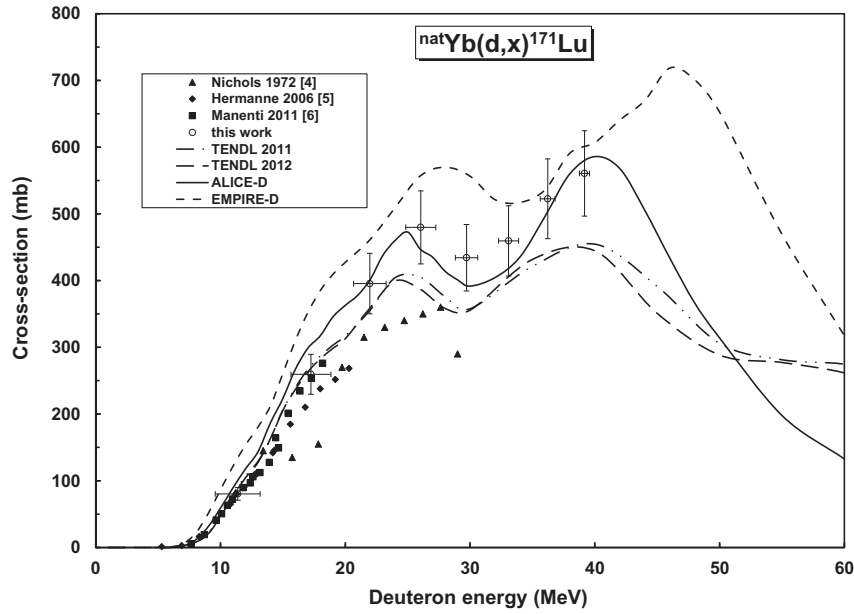


Fig. 5. Excitation function of the $^{nat}\text{Yb}(d,xn)^{171}\text{Lu}$ process.

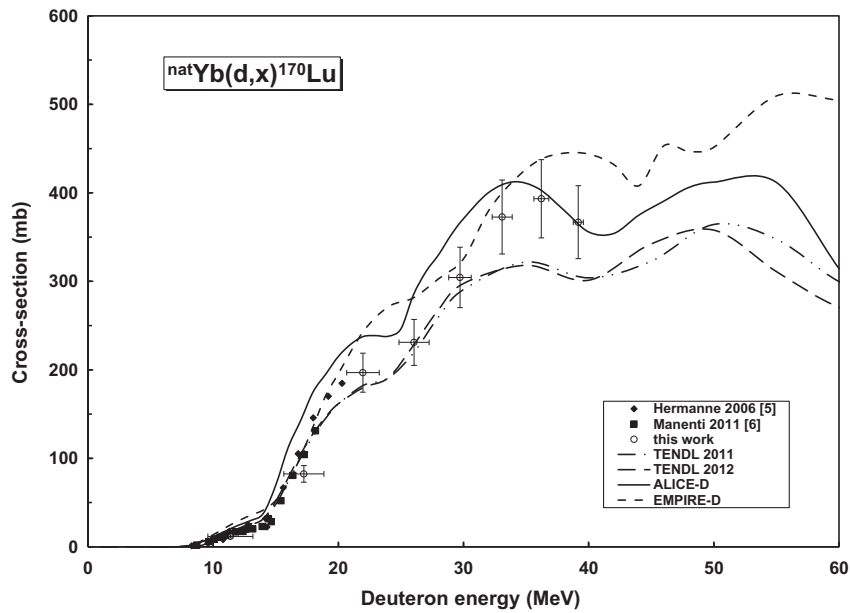


Fig. 6. Excitation function of the $^{nat}\text{Yb}((d,xn)^{170}\text{Lu}$ process.

small and cannot be distinguished on Fig. 3. The $^{173}\text{Yb}(d,2n)$ and $^{174}\text{Yb}(d,3n)$ produce the first maximum and the $^{176}\text{Yb}(d,5n)$ reaction the second one (Fig. 3). The agreement with the earlier experimental data of Hermanne et al. [5] and Manenti et al. [6] is acceptable good, but there is significant disagreement with the results of Nichols et al. [4]. It is difficult to judge the agreement with the TENDL predictions: at the low energy maximum it seems to be good, but at higher energies the experimental data are higher. ALICE-D and EMPIRE-D runs together with the TALYS results up to 15 MeV, at the maximum both give higher values, and at higher energies give similar results again.

5.1.3. $^{nat}\text{Yb}(d,xn)^{172}\text{Lu}$

The acceptable agreement of the experimental and theoretical excitation functions for ^{172}Lu production is shown in Fig. 4. Reac-

tions on five stable Yb isotopes are contributing (see Table 1). The cross-sections contain the complete contribution of the decay of short-lived isomeric state (3.7 min). The large maximum arises from contribution of the $(d,4n)$ reaction on high abundance ^{174}Yb . Our new experimental data show good agreement with the earlier results and give new data above 30 MeV. The both TENDL curves run almost together giving good description of the experimental results in the studied energy domain, while ALICE-D shows a larger maximum and EMPIRE-D overestimates above 15 MeV.

5.1.4. $^{nat}\text{Yb}(d,xn)^{171}\text{Lu}$

Below 30 MeV a good agreement of the available experimental data and the theoretical results was obtained (see Fig. 5) for cumulative production of ^{171}Lu (8.24 d) (including complete decay through isomeric transition of the short-lived (79 s) isomeric

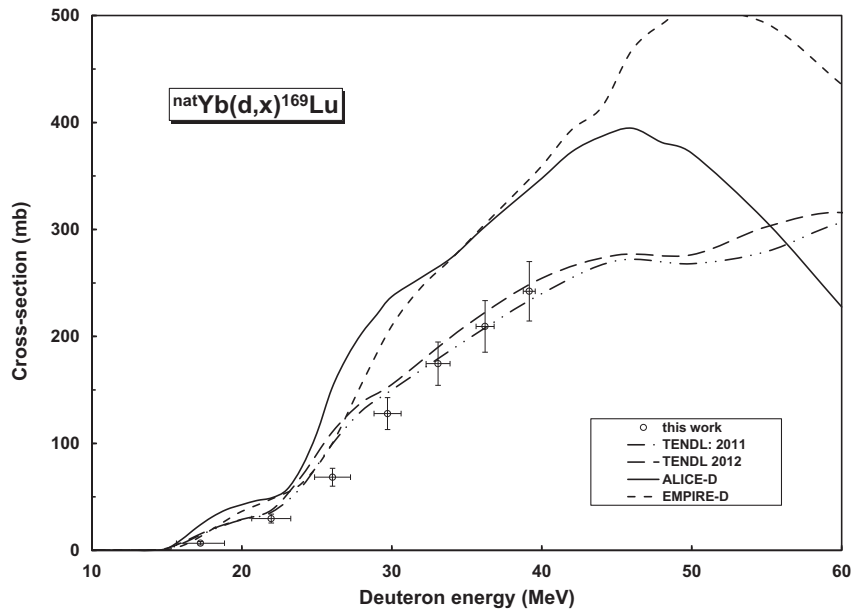


Fig. 7. Excitation function of the $^{nat}\text{Yb}(d,x)^{169}\text{Lu}$ process.

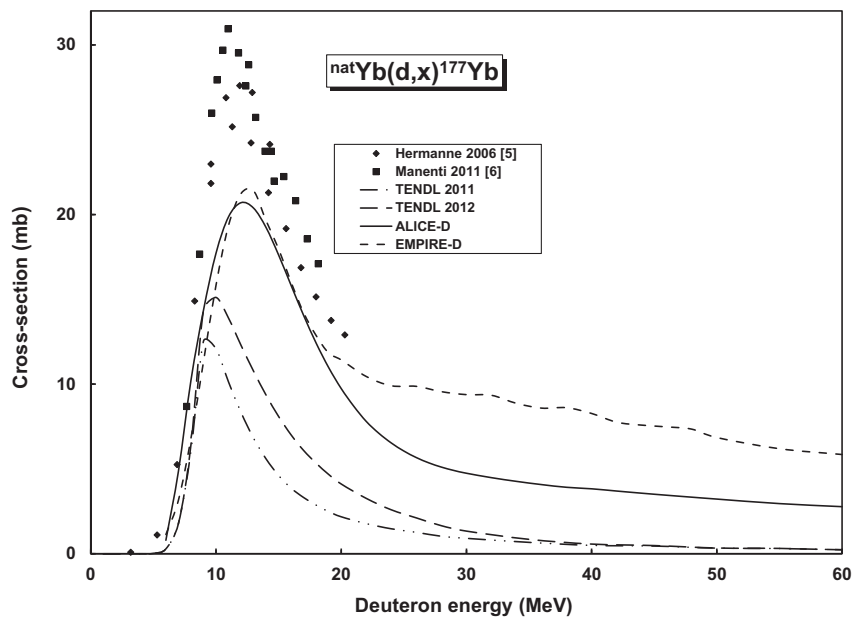


Fig. 8. Excitation function of the $^{176}\text{Yb}(d,p)^{177}\text{Yb}$ process.

state), but our values are systematically higher at higher energies. The three maxima can be connected to the reactions on respectively the low mass ytterbium isotopes, to the ^{174}Yb and to the ^{176}Yb target isotopes. Our new data agree well with those of Hermanne [5] and Manenti [6] up to 20 MeV and significantly larger than Nichols' results above 20 MeV. The local maxima are also reproduced well. Now the best approximation is given by the ALICE-D code. The TENDL results are also acceptable under 20 MeV. EMPIRE-D overestimates the experimental data in the whole energy region.

5.1.5. $^{nat}\text{Yb}(d,xn)^{170}\text{Lu}$

The excitation function for production of ^{170}Lu (2.012 d) is shown in Fig. 6. ^{170}Lu has no isomeric state, so the presented results are direct cross-sections of the ground-state, resulted in from

(d,xn) reactions on different Yb stable isotopes ($M = 170-174$). Our new data agree acceptable well with the result of earlier experiments below 20 MeV. The excitation functions predicted in the TENDL show also a good agreement with the experiment. It is difficult to distinguish between the results of the different model calculations, while they mostly run together. Only above 30 MeV is obvious that both TENDL data underestimate the experimental results.

5.1.6. $^{nat}\text{Yb}(d,xn)^{169}\text{Lu}$

No earlier experimental data were found for production of ^{169}Lu (32.018 d), probably due to the high effective reaction threshold not covered in the energy range in [5,6]. The TENDL results reproduce excellently the experimental data (Fig. 7), while both EMPIRE-D and ALICE-D overestimate significantly above 20 MeV.

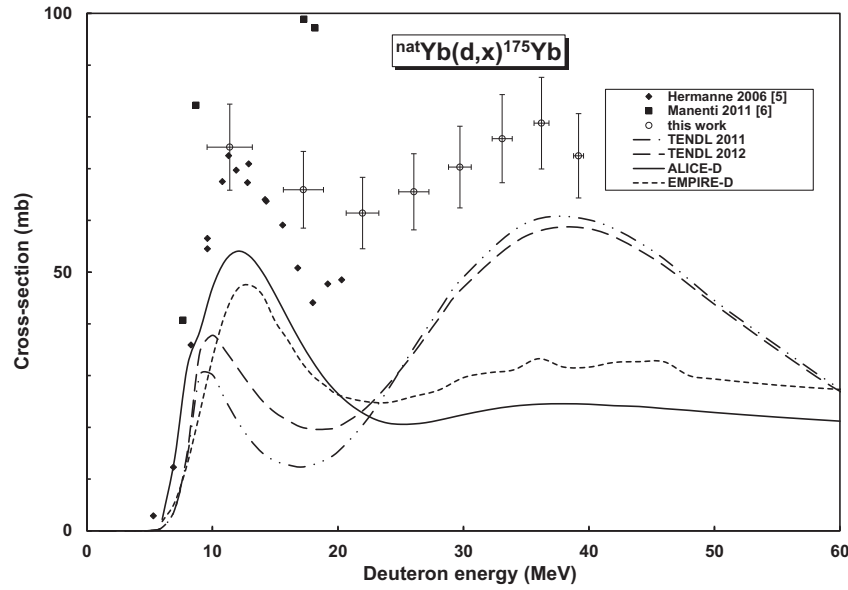


Fig. 9. Excitation function of the $^{nat}\text{Yb}(d,x)^{175}\text{Yb}$ process.

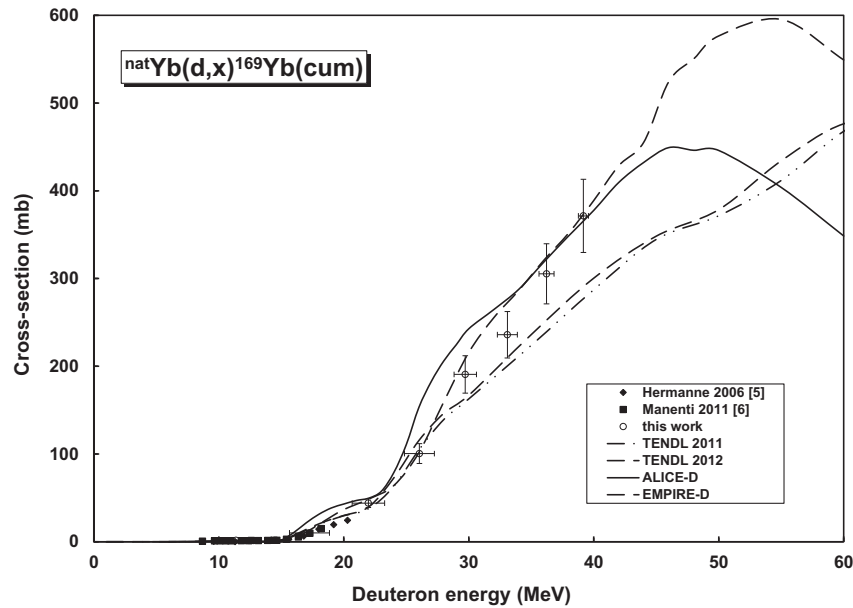


Fig. 10. Excitation function of the $^{nat}\text{Yb}(d,x)^{169}\text{Yb}$ process.

5.2. Cross-sections of ytterbium radioisotopes

The radioisotopes of Yb can be formed through two routes: directly via (d,pxn) reactions and by decay of simultaneously produced parent radioisotopes of Lu and Tm with the same mass.

5.2.1. $^{176}\text{Yb}(d,p)^{177}\text{Yb}$ process

Due to the long waiting time (around 20 h) after EOB before the first measurement we could not identify the γ -lines of the ^{177}Yb (1.911 h) in the spectra. To illustrate the poor predictivity of the model codes for the (d,p) reactions, in Fig. 8 we have compared the experimental data of [5,6] with the TALYS results in the TENDL libraries. The disagreement in the maximum value is around a factor of two. The results of model calculations still significantly underestimate the experimental data, although new improvements for description of (d,p) reactions were implemented in the

TALYS code. Phenomenological systematics of the (d,p) cross-sections and the problems of the theoretical descriptions are discussed in more detail in [25,26].

5.2.2. $^{nat}\text{Yb}(d,x)^{175}\text{Yb}$ process

Fig. 9 shows the cross-sections for cumulative production of ^{175}Yb (4.185 d) via direct (d,pxn) reactions and from decay of ^{175}Tm (15.2 min) produced by the $^{176}\text{Yb}(d,2pn)$ process. According to the theory and to the systematics the $(d,2pn)$ contribution is small. Therefore the cumulative cross-sections mostly reflect the direct (d,pxn) cross-sections. Our present data above 20 MeV are new, in the overlapping region show agreement with the data of Hermanne [5]. The earlier results of Manenti [6] are higher. Similar to the previous case the theoretical results strongly underestimate these processes; the form of the excitation function is reproduced by TALYS only.

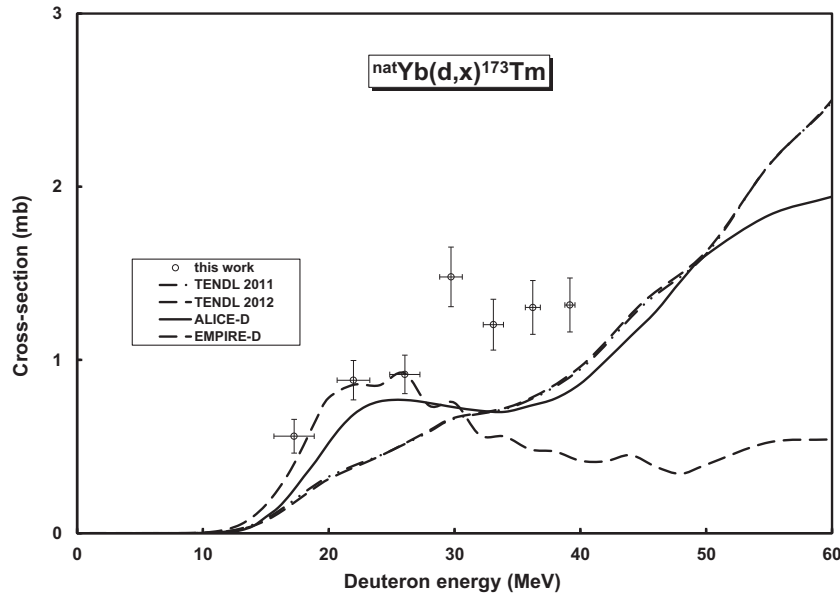


Fig. 11. Excitation function of the $^{nat}\text{Yb}(d,x)^{173}\text{Tm}$ process.

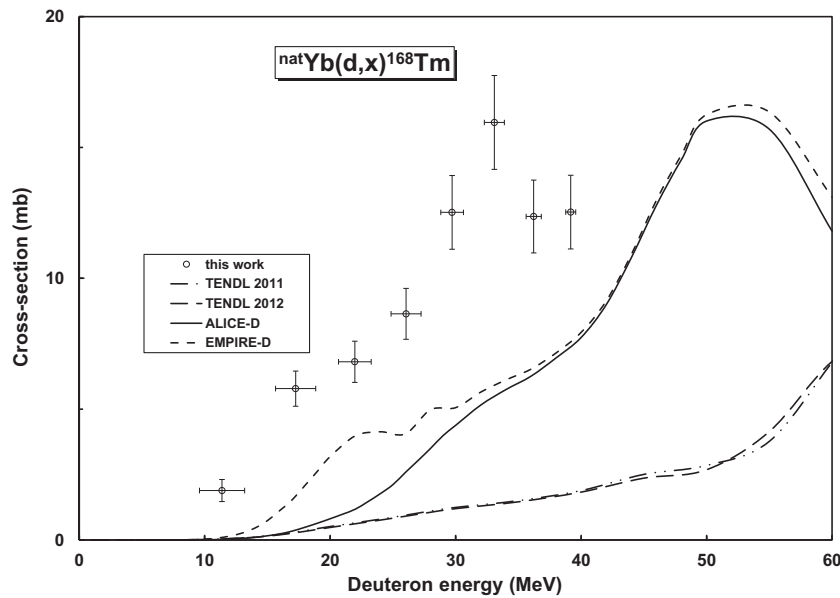


Fig. 12. Excitation function of the $^{nat}\text{Yb}(d,x)^{168}\text{Tm}$ process.

5.2.3. $^{nat}\text{Yb}(d,x)^{169}\text{Yb}$

The isotope ^{169}Yb ($T_{1/2} = 32.018\text{ d}$) is obtained through the direct production via (d,pxn) reactions and is also populated by decay of the simultaneously produced parent ^{169}Lu (34.06 h). The measured cumulative activation cross-sections are shown in Fig. 10. The agreement with the earlier experimental data and with TALYS, ALICE-D and EMPIRE-D results is acceptable good, although it is difficult to distinguish between the theoretical codes, while they run together up to 25 MeV. Above this energy our new experimental data are better described with ALICE-D and EMPIRE-D. The earlier experimental data of Manenti [6] and Hermance [5] are in good agreement with our new results in the overlapping energy domain.

5.3. Cross-sections of residual radioisotopes of thulium

The radioisotopes of thulium are produced directly via $(d,2pxn)$ reactions, and/or through decay of simultaneously formed parent

Lu and Yb radionuclides. For direct production at low energies the α -particle emission dominates the possible $(p,2pxn)$ ($x \geq 2$) reaction channels. At higher energies the individual particle emission is more significant. The small contributions from the β^- -decay of erbium radioisotopes can be neglected due to the low probability of the $(d,3pxn)$ processes.

5.3.1. $^{nat}\text{Yb}(d,x)^{173}\text{Tm}$

According to the Fig. 11 the agreement of the experimental and theoretical data for the directly produced ^{173}Tm (8.24 h) is not too bad, especially under 30 MeV, taking into account the complex particle emissions for production of this radionuclide.

5.3.2. $^{nat}\text{Yb}(d,x)^{168}\text{Tm}$

The measured excitation function for production of ^{168}Tm (93.1 d) is shown in Fig. 12. The theory significantly underestimates the experimental values. The both TENDL calculations run together,

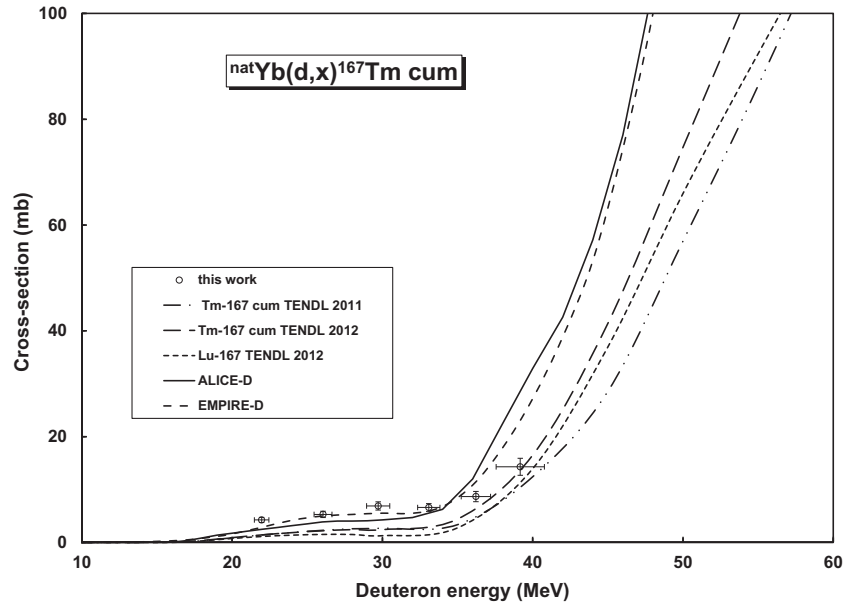


Fig. 13. Excitation function of the ${}^{\text{nat}}\text{Yb}(d,x){}^{167}\text{Tm}$ process.

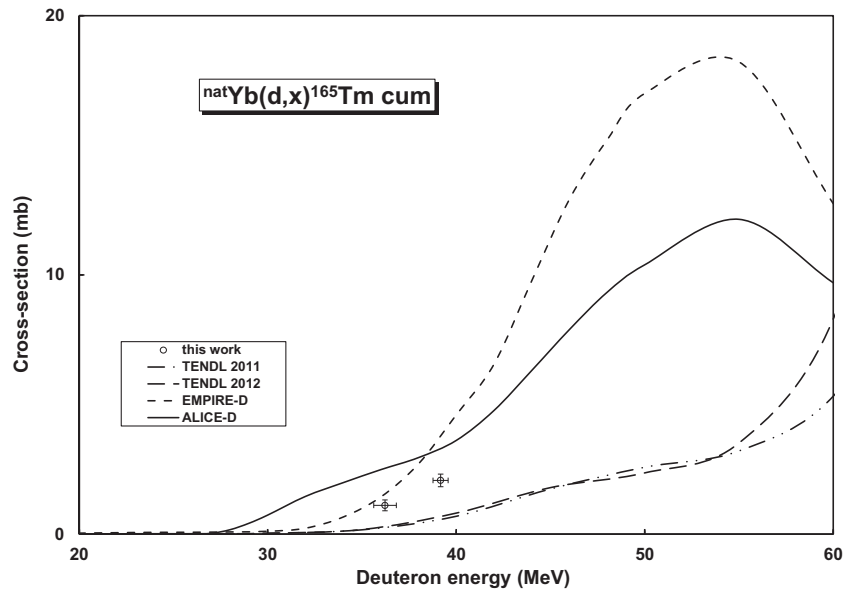


Fig. 14. Excitation function of the ${}^{\text{nat}}\text{Yb}(d,x){}^{165}\text{Tm}$ process.

there are no improvements between the 2011 and 2012 versions. EMPIRE-D and ALICE-D give similar, but still underestimating results.

5.3.3. ${}^{\text{nat}}\text{Yb}(d,x){}^{167}\text{Tm}$

The radionuclide ${}^{167}\text{Tm}$ (9.25 d) is produced directly and from the decay of short-lived parent ${}^{167}\text{Yb}$ (17.5 min). According to Table 1 and to Fig. 13, the threshold for production of the ${}^{167}\text{Tm}$ is high in the investigated energy range, but the cross-sections are small.

We present cross-sections for cumulative production, after complete decay of ${}^{167}\text{Lu}$. The resulted cross-sections contain large uncertainties, especially near the effective threshold, due to the need of correction for interference in the γ -ray signal of ${}^{167}\text{Tm}$.

The two measurable γ -lines of ${}^{167}\text{Tm}$ have energies of 207.801(42%) and 531.54 keV (1.61%). As it was mentioned earlier the 207.8 keV line overlaps with the 208.3662 keV γ -line of ${}^{177g}\text{Lu}$, which is experimentally practically inseparable because of the en-

ergy resolution of the used detector. Therefore we have tried to use the 532 keV γ -line of ${}^{167}\text{Tm}$ with limited success (low count rates, large scattering). Therefore we have separated the contribution of ${}^{177g}\text{Lu}$ in the γ -spectra measured 20 day after EOB. It was possible due to the lower γ -abundance of the 208 keV γ -line of ${}^{177}\text{Lu}$, due to the shorter half-life and to the relatively low cross-sections for cumulative production of ${}^{177g}\text{Lu}$ on natural Yb. The experimental excitation function for ${}^{\text{nat}}\text{Yb}(d,x){}^{177\text{cum}}\text{Lu}$ (discussed in Section 5.1.1) is also shown in Fig. 13. It is difficult to distinguish, which model code gives the better results, but at least at lower energies under 35 MeV the approximations of EMPIRE-D and ALICE-D are better, but above this energy the experimental values reach the TENDL 2012 curve.

5.3.4. ${}^{\text{nat}}\text{Yb}(d,x){}^{165}\text{Tm}$

The ${}^{165}\text{Tm}$ (30.06 h) is produced both directly through ${}^{\text{nat}}\text{Yb}(d,pxn)$ reactions and indirectly from decay of short lived parent ${}^{165}\text{Yb}$ (9.9 min). The effective threshold is close to our

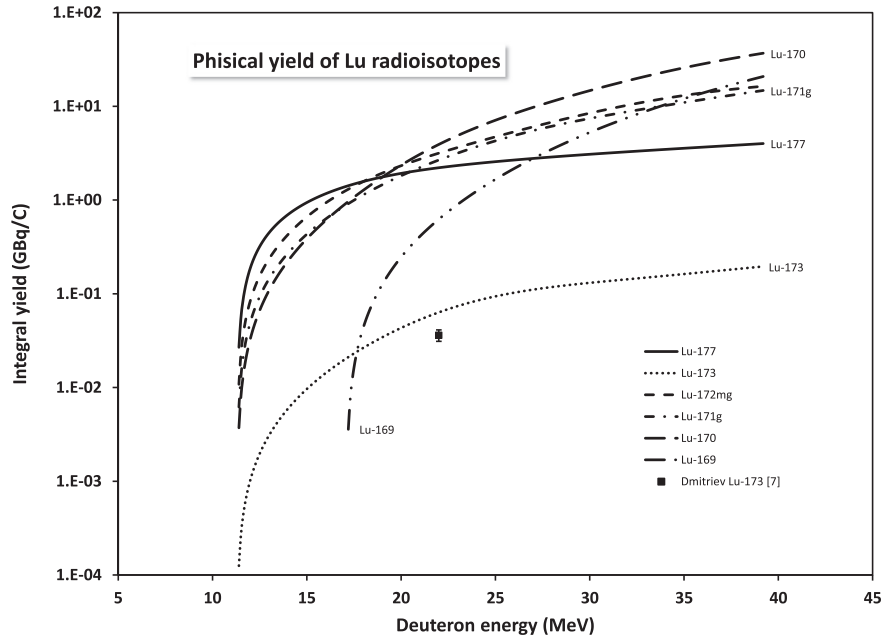


Fig. 15. Integral yields for production of Lu radioisotopes.

Table 2

Measured cross-sections of the $^{nat}\text{Yb}(d,xn)^{177,173,172\text{mg},171\text{mg},170,169}\text{Lu}$ reactions.

| Energy $\pm dE$ (MeV) | | Cross-section $\pm d\sigma$ (mb) | | | | | | | | | | | |
|-----------------------|-----|----------------------------------|------|-------------------|------|---------------------------|------|---------------------------|------|-------------------|------|-------------------|------|
| | | ^{177}Lu | | ^{173}Lu | | $^{172\text{g}}\text{Lu}$ | | $^{171\text{g}}\text{Lu}$ | | ^{170}Lu | | ^{169}Lu | |
| 39.2 | 0.4 | 52.0 | 10.8 | 296.1 | 36.2 | 288.0 | 33.0 | 560.6 | 63.9 | 366.8 | 41.2 | 242.2 | 27.8 |
| 36.2 | 0.6 | 47.6 | 12.6 | 277.9 | 34.9 | 374.7 | 42.7 | 522.6 | 59.7 | 393.4 | 44.2 | 209.4 | 24.1 |
| 33.1 | 0.8 | 51.8 | 14.0 | 246.4 | 33.4 | 482.5 | 57.7 | 459.6 | 52.7 | 372.7 | 41.8 | 174.5 | 20.3 |
| 29.7 | 0.9 | 54.1 | 15.5 | 253.7 | 31.2 | 450.2 | 51.2 | 434.3 | 49.8 | 304.4 | 34.2 | 127.9 | 15.0 |
| 26.0 | 1.2 | 71.0 | 24.9 | 386.5 | 45.3 | 377.7 | 43.0 | 479.8 | 54.7 | 231.0 | 25.9 | 68.4 | 8.4 |
| 22.0 | 1.3 | 79.4 | 23.0 | 557.3 | 65.1 | 278.3 | 31.9 | 395.5 | 45.2 | 196.8 | 22.1 | 29.7 | 4.2 |
| 17.2 | 1.6 | 182.7 | 59.2 | 377.1 | 44.8 | 253.5 | 29.0 | 259.4 | 30.0 | 82.4 | 9.3 | 6.7 | 1.6 |
| 11.4 | 1.8 | 286.3 | 43.7 | 98.9 | 13.7 | 106.1 | 12.2 | 80.4 | 9.5 | 11.8 | 1.7 | | |

Table 3

Measured cross-sections of the $^{nat}\text{Yb}(d,x)^{175,169}\text{Yb}$ and $^{nat}\text{Yb}(d,x)^{173,172,168,167,165}\text{Tm}$ reactions.

| Energy $\pm dE$ (MeV) | | Cross-section $\pm d\sigma$ (mb) | | | | | | | | | | | |
|-----------------------|-----|----------------------------------|-----|-------------------|------|-------------------|-----|-------------------|-----|-------------------|-----|-------------------|-----|
| | | ^{175}Yb | | ^{169}Yb | | ^{173}Tm | | ^{168}Tm | | ^{167}Tm | | ^{165}Tm | |
| 39.2 | 0.4 | 72.5 | 8.2 | 371.4 | 41.7 | 1.3 | 0.2 | 12.5 | 1.4 | 14.3 | 1.6 | 2.1 | 0.2 |
| 36.2 | 0.6 | 78.8 | 8.9 | 305.4 | 34.3 | 1.3 | 0.2 | 12.4 | 1.4 | 8.7 | 1.0 | 1.1 | 0.2 |
| 33.1 | 0.8 | 75.8 | 8.5 | 236.0 | 26.5 | 1.2 | 0.2 | 16.0 | 1.8 | 6.6 | 0.7 | | |
| 29.7 | 0.9 | 70.3 | 7.9 | 190.7 | 21.4 | 1.5 | 0.2 | 12.5 | 1.4 | 6.9 | 0.8 | | |
| 26.0 | 1.2 | 65.5 | 7.4 | 100.5 | 11.3 | 0.9 | 0.1 | 8.6 | 1.0 | 5.3 | 0.6 | | |
| 22.0 | 1.3 | 61.4 | 6.9 | 44.0 | 4.9 | 0.9 | 0.1 | 6.8 | 0.8 | 4.3 | 0.5 | | |
| 17.2 | 1.6 | 65.9 | 7.4 | 10.0 | 1.1 | 0.6 | 0.1 | 5.8 | 0.7 | | | | |
| 11.4 | 1.8 | 74.2 | 8.3 | 1.5 | 0.3 | | | 1.9 | 0.4 | | | | |

maximum energy. The few measured cross-section points are shown in Fig. 14.

6. Integral yields

On the basis of our new experimental cross-section data and the results of the model calculations we determined integral yields for production of the investigated reaction products. The results are so called physical yields [27] corresponding to instantaneous short irradiation. The calculated yields for $^{nat}\text{Yb}(d,xn)^{177,173,172\text{mg},171\text{mg},170,169}\text{Lu}$, $^{nat}\text{Yb}(d,x)^{175,169}\text{Yb}$ and $^{nat}\text{Yb}(d,x)^{173,172,168,167,165}\text{Tm}$ are shown in Figs. 15 and 16 in comparison with the few experimental integral thick target yield data found in the literature. Dmitriev et al. reported radioactive thick

target nuclide yields at 22 MeV incident deuteron energy [7] for the $^{nat}\text{Yb}(d,x)^{173}\text{Lu}$ and $^{nat}\text{Yb}(d,x)^{174\text{g}}\text{Lu}$ reactions. Our calculated yield curve for ^{173}Lu runs above the data point of Dmitriev at 22 MeV.

7. Summary and conclusion

Twelve excitation functions of deuteron induced nuclear reactions on Yb were measured up to 40 MeV. All data above 20 MeV, except for production of $^{171,172,173}\text{Lu}$ were measured for the first time. The experimental data were compared with the results of EMPIRE-D and ALICE-D calculations and data in the TENDL 2011 and 2012 libraries based on TALYS results. The theoretical calculations describe the shape and the absolute values of the experimen-

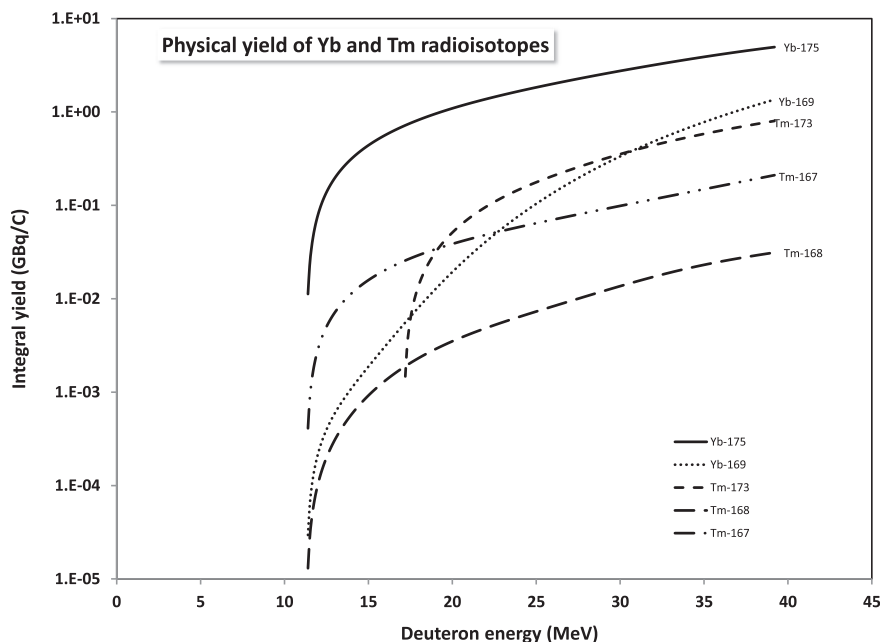


Fig. 16. Integral yields for production of Yb and Tb radioisotopes.

tal data only with moderate success, and the (d,p) reaction is especially significantly underestimated by the theory. Further improvement of the used model codes is required. The comparison with the low energy earlier experimental data shows excellent agreement.

The obtained experimental data provide a basis for improved model calculations and for different applications in the field of nuclear medicine and for estimating production yields of long-lived products for dose estimations and waste handling.

Presently the ytterbium has very few industrial uses, but the applications are growing (in laser technology, fiber optic technologies, etc.).

Among the radioactive nuclear reaction products ^{177}Lu [28–31], ^{172}Lu [32–34], ^{169}Yb [35], ^{175}Yb [36] and ^{167}Tm [37] have potential relevance in nuclear medicine for cancer treatment and as tracer in nuclear biology (for a review see [38]).

In the domain of industrial applications, the γ -emitter ^{169}Yb (39 d half-life) has been used in sealed sources for industrial applications, for substitution of ^{192}Ir sources applied in conventional non-destructive testing (NDT) projectors, providing better quality of the radiographic pattern [39].

The longer lived $^{173,174}\text{Lu}$ are used as radioactive tracers in different processes [40,41] and the ^{172}Lu (^{172}Yb) decay is used for investigation ion implantation in semiconductors by using PAC technique [42], and for radiotracer studies of oil pipeline flow rates, refinery column residence times, and the performance of a coal liquefaction pilot plant [43].

Deuteron induced reactions on ytterbium however, are not the most favorable reactions for production of some of these radionuclides as for instance ^{169}Yb , ^{177}Lu and ^{175}Yb can be produced much more economically at reactors via (n,γ) reactions. The optimal routes for the production of ^{167}Tm are the $^{167}\text{Er}(p,n)$ [44] and $^{167}\text{Er}(d,2n)$ [23].

Acknowledgements

This work was done in the frame of MTA-JSPS and MTA-FWO (Vlaanderen) research projects. The authors acknowledge the support of research projects and of their respective institutions in providing the materials and the facilities for this work.

References

- [1] F. Tárkányi, A. Hermanne, S. Takács, F. Ditrói, B. Király, H. Yamazaki, M. Baba, A. Mohammadi, A.V. Ignatyuk, Activation cross sections of proton induced nuclear reactions on ytterbium up to 70 MeV, Nucl. Instr. Meth. B 267 (2009) 2789–2801.
- [2] F. Tárkányi, A. Hermanne, S. Takács, F. Ditrói, B. Király, H. Yamazaki, M. Baba, A. Mohammadi, A.V. Ignatyuk, Activation cross sections of the Yb-nat(p, xn)Lu-169 reaction for indirect production of the therapeutic radionuclide Yb-169, Nucl. Instr. Meth. B 267 (2009) 2802–2807.
- [3] B. Király, F. Tárkányi, S. Takács, A. Hermanne, S.F. Kovalev, A.V. Ignatyuk, Excitation functions of alpha-particle induced nuclear reactions on natural ytterbium, Nucl. Instr. Meth. B 266 (2008) 3919–3926.
- [4] A. Nichols, Excitation functions for the formation of various gadolinium and lutetium isotopes by (d, xn) reactions, in: AERE-R-6965, Atomic Energy Research Establishment, Harwell(England), 1972.
- [5] A. Hermanne, S. Takács, M.B. Goldberg, E. Lavie, Y.N. Shubin, S. Kovalev, Deuteron-induced reactions on Yb: Measured cross sections and rationale for production pathways of carrier-free, medically relevant radionuclides, Nucl. Instr. Meth. B 247 (2006) 223–231.
- [6] S. Manenti, F. Groppi, A. Gandini, L. Gini, K. Abbas, U. Holzwarth, F. Simonelli, M. Bonardi, Excitation function for deuteron induced nuclear reactions on natural ytterbium for production of high specific activity Lu-177g in no-carrier-added form for metabolic radiotherapy, Appl. Radiat. Isotopes 69 (2011) 37–45.
- [7] P.P. Dmitriev, N.N. Krasnov, G.A. Molin, Radioactive nuclide yields for thick target at 22 MeV deuterons energy, Yadernie Konstanti 34 (1982) 38.
- [8] A.I. Dityuk, A.Y. Konobeyev, V.P. Lunev, Y.N. Shubin, New version of the advanced computer code ALICE-IPPE, in: INDC (CCP)-410, IAEA, Vienna, 1998.
- [9] A.J. Koning, S. Hilaire, M.C. Duijvestijn, TALYS-1.0, in: O. Bersillon, F. Gunsing, E. Bauge, R. Jacqmin, S. Leray (Eds.), International Conference on Nuclear Data for Science and Technology, EDP Sciences, Nice, France, 2007, p. 211.
- [10] A.J. Koning, D. Rochman, TALYS-based Evaluated Nuclear Data Library Version 4, in: <http://www.talys.eu/tendl-2012/>, Nuclear Research and Consultancy Group (NRG), Petten, The Netherlands, 2011.
- [11] N. Soppera, M. Bossant, E. Dupont, H. Henriksson, Y. Rugama, Recent upgrades to the nuclear data tool JANIS, J. Korean Phys. Soc. 59 (2011) 1329–1332.
- [12] F. Ditrói, F. Tárkányi, S. Takács, A. Hermanne, H. Yamazaki, M. Baba, A. Mohammadi, A.V. Ignatyuk, Study of activation cross-sections of deuteron induced reactions on rhodium up to 40 MeV, Nucl. Instr. Meth. B 269 (2011) 1963–1972.
- [13] F. Ditrói, F. Tárkányi, S. Takács, A. Hermanne, H. Yamazaki, M. Baba, A. Mohammadi, A.V. Ignatyuk, Activation cross-sections of deuteron induced nuclear reactions on manganese up to 40 MeV, Nucl. Instr. Meth. B 269 (2011) 1878–1883.
- [14] F. Tárkányi, F. Ditrói, A. Hermanne, S. Takács, B. Király, H. Yamazaki, M. Baba, A. Mohammadi, A.V. Ignatyuk, Activation cross-sections of deuteron induced nuclear reactions on gold up to 40 MeV, Nucl. Instr. Meth. B 269 (2011) 1389–1400.

- [15] F. Tárkányi, F. Ditrói, S. Takács, B. Király, A. Hermanne, M. Sonck, M. Baba, A.V. Ignatyuk, Investigation of activation cross-sections of deuteron induced nuclear reactions on ^{98}Mo up to 50 MeV, Nucl. Instr. Meth. B 274 (2012) 1–25.
- [16] Kinsey R.R., C.I. Dunford, J.K. Tuli, T.W. Burrows, NUDAT 2.6, in: Capture Gamma Ray Spectroscopy and Related Topics, Springer Hungarica Ltd., Budapest, 1997, p. p. 657.
- [17] F. Tárkányi, S. Takács, K. Gul, A. Hermanne, M.G. Mustafa, M. Nortier, P. Oblozinsky, S.M. Qaim, B. Scholten, Y.N. Shubin, Z. Youxiang, Beam monitor reactions. Charged particle cross-section database for medical radioisotope production: diagnostic radioisotopes and monitor reactions, in: TECDOC 1211, IAEA, 2001, p. 49. Chapter 4.
- [18] B. Pritychenko, A. Sonzogni, Q-value Calculator, NNDC, Brookhaven National Laboratory, 2003.
- [19] H.H. Andersen, J.F. Ziegler, Hydrogen Stopping Powers and Ranges in all Elements, The Stopping and Ranges of Ions in Matter, vol. 3, Pergamon Press, New York, 1977.
- [20] F. Tárkányi, F. Szelecsényi, S. Takács, Determination of effective bombarding energies and fluxes using improved stacked-foil technique, Acta Radiol. Suppl. 376 (1991) 72.
- [21] International-Bureau-of-Weights-and-Measures, Guide to the expression of uncertainty in measurement, 1st ed., International Organization for Standardization, Genève, Switzerland, 1993.
- [22] M. Herman, R. Capote, B.V. Carlson, P. Oblozinsky, M. Sin, A. Trkov, H. Wienke, V. Zerkin, EMPIRE: nuclear reaction model code system for data evaluation, Nucl. Data Sheets 108 (2007) 2655–2715.
- [23] F. Tárkányi, A. Hermanne, S. Takács, F. Ditrói, I. Spahn, S.F. Kovalev, A.V. Ignatyuk, S.M. Qaim, Activation cross sections of the Tm-169($d,2n$) reaction for production of the therapeutic radionuclide Yb-169, Appl. Radiat. Isotopes 65 (2007) 663–668.
- [24] F. Tárkányi, A. Hermanne, S. Takács, K. Hilgers, S.F. Kovalev, A.V. Ignatyuk, S.M. Qaim, Study of the $^{192}\text{Os}(d,2n)$ reaction for, production of the therapeutic radionuclide ^{192}Ir in no-carrier added form, Appl. Radiat. Isotopes 65 (2007) 1215–1220.
- [25] A.V. Ignatyuk, Phenomenological systematics of the (d,p) cross sections, <http://www-nds.iaea.org/fendl3/000pages/RCM3/slides/Ignatyuk_FENDL-3%20presentation.pdf>, in: IAEA (Ed.), Vienna, 2011.
- [26] E. Simeckova, P. Bem, M. Honusek, M. Stefanik, U. Fischer, S.P. Simakov, R.A. Forrest, A.J. Koning, J.C. Sublet, M. Avrigeanu, F.L. Roman, V. Avrigeanu, Low and medium energy deuteron-induced reactions on Cu-63, Cu-65 nuclei, Phys. Rev. C 84 (2011) 14605.
- [27] M. Bonardi, The contribution to nuclear data for biomedical radioisotope production from the Milan cyclotron facility, in: K. Okamoto (Ed.), Consultants Meeting on Data Requirements for Medical Radioisotope Production, IAEA, INDC(NDS)-195 (1988), Tokyo, Japan, 1987, p. 98.
- [28] M. deJong, W.A. Breeman, R. Valkema, B.F. Bernard, E.P. Krenning, Combination radionuclide therapy using ^{177}Lu - and ^{90}Y -labeled somatostatin analogs, J. Nucl. Med. 46 (Supplement) (2005) 13S–17S.
- [29] J.J. Teunissen, D.J. Kwekkeboom, E.P. Krenning, Quality of life in patients with gastroenteropancreatic tumors treated with [^{177}Lu -DOTA0, Tyr3]octreotate, J. Clin. Oncol. 22 (2004) 2724–2729.
- [30] R.B. Michel, P.M. Andrews, A.V. Rosario, D.M. Goldenberg, M.J. Mattes, Lu-177-antibody conjugates for single-cell kill of B-lymphoma cells in vitro and for therapy of micrometastases in vivo, Nucl. Med. Biol. 32 (2005) 269–278.
- [31] S. Vallabhajosula, I. Kuji, K.A. Hamacher, S. Konishi, L. Kostakoglu, P.A. Kothari, M.I. Milowski, D.M. Nanus, N.H. Bander, S.J. Goldsmith, Pharmacokinetics and biodistribution of In-111-Lu-177-labeled J591 antibody specific for prostate-specific membrane antigen: Prediction of Y-90-J591 radiation dosimetry based on In-111 or Lu-177, J. Nucl. Med. 46 (2005) 634–641.
- [32] R.J. Daniels, P.M. Grant, H.A. Obrien, Production, Recovery, and Purification of Hf-172 for Utilization in Nuclear-Medicine as Generator of Lu-172, Int. J. Nucl. Med. Biol. 5 (1978) 11–17.
- [33] S.K. Das, A.G.C. Nair, R.K. Chatterjee, R. Guin, S.K. Saha, The performance of a new Hf-172-Lu-172 generator, Appl. Radiat. Isotopes 47 (1996) 643–644.
- [34] M. Sadeghi, M. Enferadi, H. Nadi, Study of the cyclotron production of Lu-172: an excellent radiotracer, J. Radioanal. Nucl. Ch 286 (2010) 259–263.
- [35] P. Fan, S. Chiu-Tsao, N. Patel, K. Ravi, W. Sherman, J. Pisch, L.B. Harrison, H.S. Tsao, Yb-169: a promising new isotope for intravascular brachytherapy, Cardiovasc. Radiat. Med. 2 (2001) 52–53.
- [36] S. Chakraborty, P.R. Unni, M. Venkatesh, M.R. Pillai, Feasibility study for production of ^{175}Yb : a promising therapeutic radionuclide, Appl. Radiat. Isotopes 57 (2002) 295–301.
- [37] J. Stepanek, B. Larsson, R. Weinreich, Auger-electron spectra of radionuclides for therapy and diagnostics, Acta Oncol. 35 (1996) 863–868.
- [38] G.-J. Beyer, H.L. Ravn, U. Köster, Perspectives for the Large Scale Production of Radiolanthanides with Medical Potential, IAEA (Ed.) Trends In Radiopharmaceuticals (ISTR-2005), IAEA, Vienna, 2005, pp. 331–338.
- [39] K.J. Son, J.S. Lee, U.J. Park, S.B. Hong, K.S. Seo, H.S. Han, Development of Miniature Radiation Sources for Medical and Non-destructive Testing Applications, in: IAEA (Ed.) TECDOC-1512, IAEA, Vienna, 2006, p. 93.
- [40] N.L. Smith, E.S. Delucchi, D.T. Mecozi, Use of radioactive tracers for selection of rare earth precipitants and ignition temperatures, in: Conference on Analytical Chemistry in Energy Technology, Lawrence Livermore Lab UCRL-83402, CONF-791049-28, Gatlinburg, TN, USA, 1979.
- [41] Z.Y. Zhang, Z.F. Chai, Isotopic tracer studies of chemical behavior of rare earth elements in environmental and biological sciences, Radiochim. Acta 92 (2004) 355–358.
- [42] R. Nedelec, R. Vanden, I. Collaboration, The rare earth PAC probe Lu-172 in wide band-gap semiconductors, Hyperfine Interact 158 (2004) 281–284.
- [43] P.M. Grant, G.E. Montero, A.M. Newman, H.A. Obrien, 1st Use of Millicurie Levels of Hf-172-Lu-172 in the Industrial Sector, J. Radioanal. Nucl. Ch Le 96 (1985) 629–633.
- [44] F. Tárkányi, A. Hermanne, S. Takács, B. Király, I. Spahn, A.V. Ignatyuk, Experimental study of the excitation functions of proton induced nuclear reactions on Er-167 for production of medically relevant Tm-167, Appl. Radiat. Isotopes 68 (2010) 250–255.